Electronic Supporting Information for

Molecular isomerism induced Fe(II) spin state difference based on tautomerization of 4(5)-methylimidazole group

*Wang-Kang Han[a], Zhi-Hua Li[a], Wei Zhu[a], Tao Li[a], Zaijun Li[a], Xuehong Ren[b] and Zhi-Guo Gu[a]**

[a] *The Key Laboratory of Food Colloids and Biotechnology, Ministry of Education, School of Chemical and Material Engineering, Jiangnan University, Wuxi 214122, P.R. China*
[b] *The Key Laboratory of Eco-textiles of Ministry of Education, College of Textiles and Clothing, Jiangnan University, Wuxi 214122, P.R. China*

E-mail: zhiguogu@jiangnan.edu.cn

1. The fast tautomerization process of 4(5)-methylimidazole-2-carbaldehyde

The tautomerization of proton transfer in 4(5)-methylimidazole group is typically a very fast process, and the peaks associated with each tautomer even could not be discernible through ^{1}H NMR.

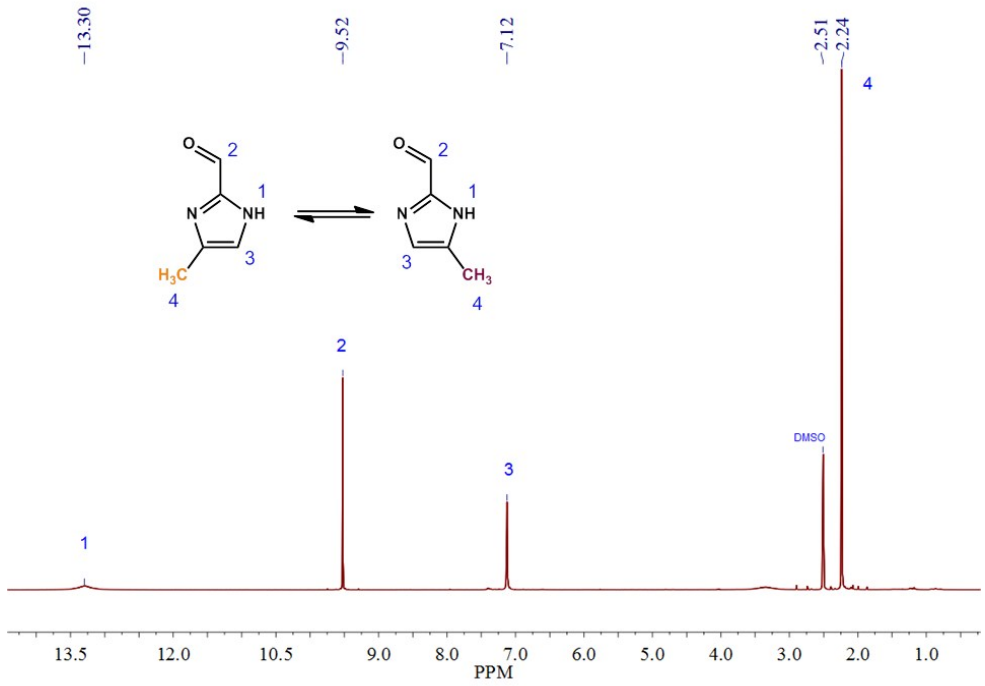

Figure. S1. ^{1}H NMR spectrum of 4(5)-methylimidazole-2-carbaldehyde.

2. Characterizations of 4(5)-MHIC

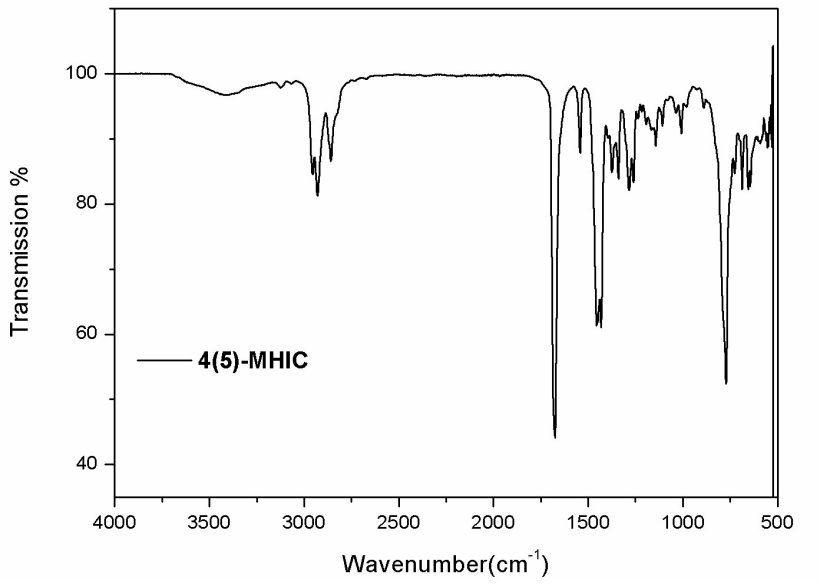

Figure. S2. ATR-FTIR spectrum of 4(5)-MHIC.

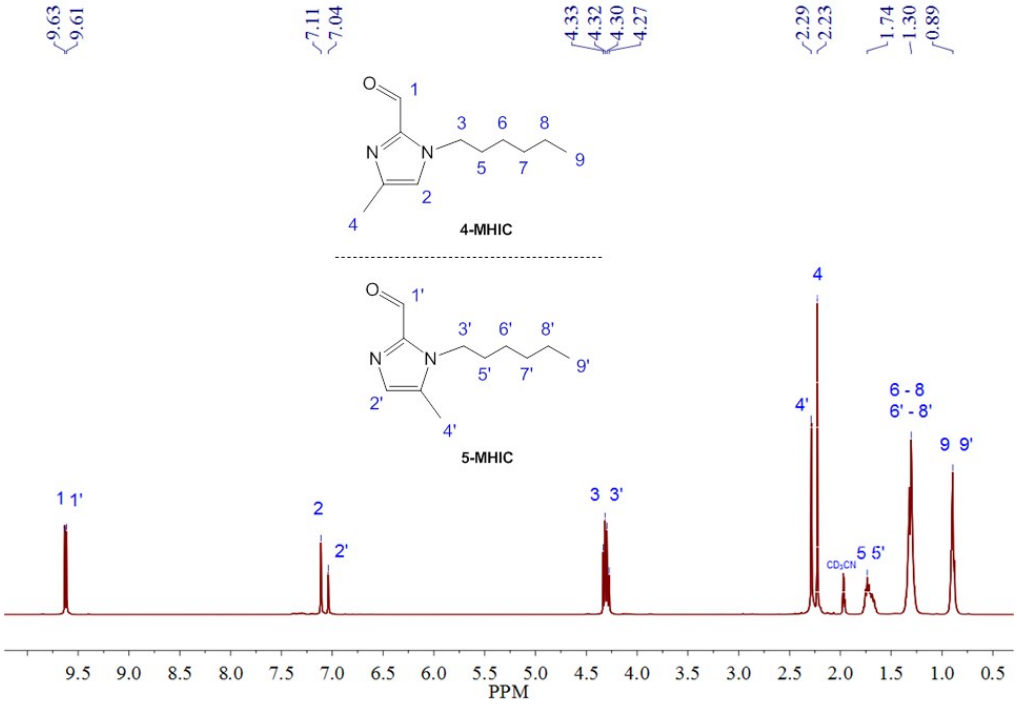

Figure. S3. ^{1}H NMR spectrum of 4(5)-MHIC.

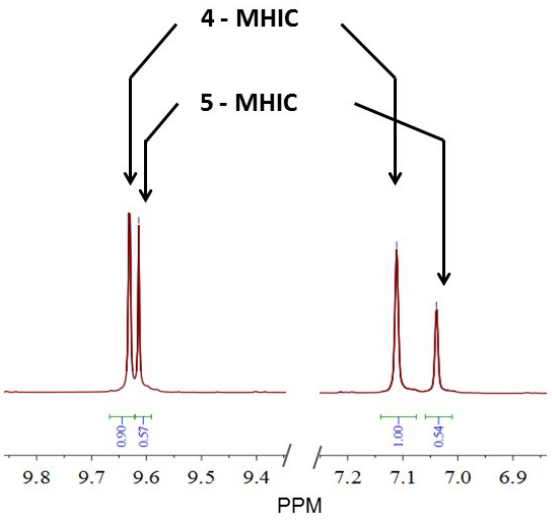

Figure. S4. Partial ^{1}H NMR spectrum for 4(5)-MHIC showing relative intensities of peaks associated with the 4-methyl and 5-methyl tautomers.

3. Infrared (IR) spectra of complexes 1a, 1b and 2

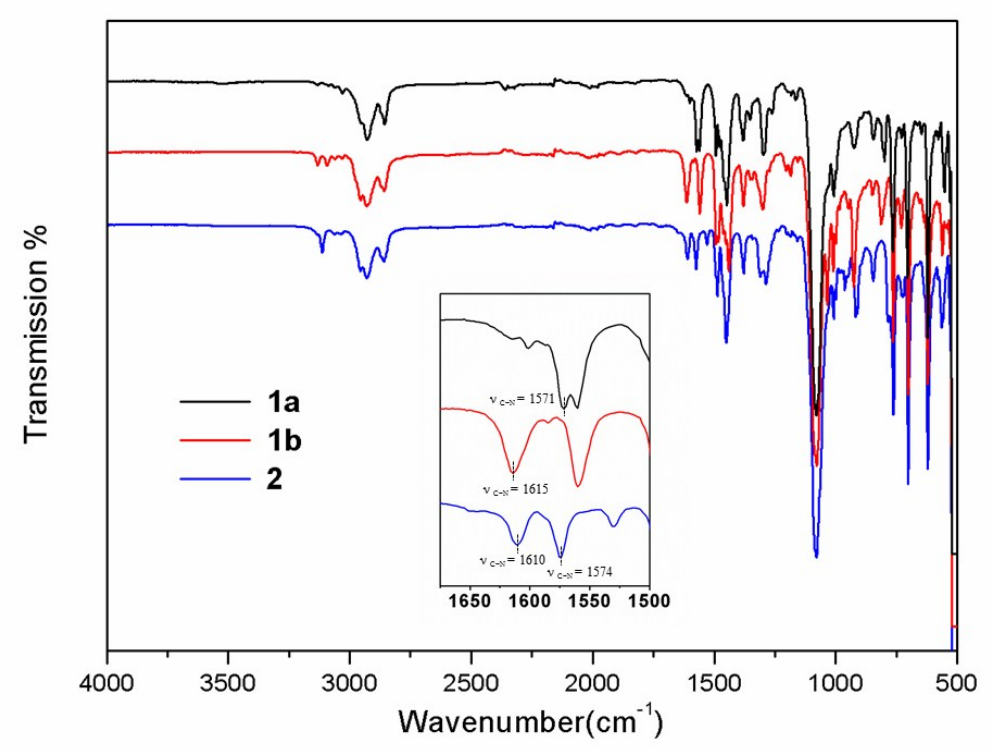

Figure. S5. ATR FT-IR spectra of **1a**, **1b** and **2**.

4. UV/Vis spectra

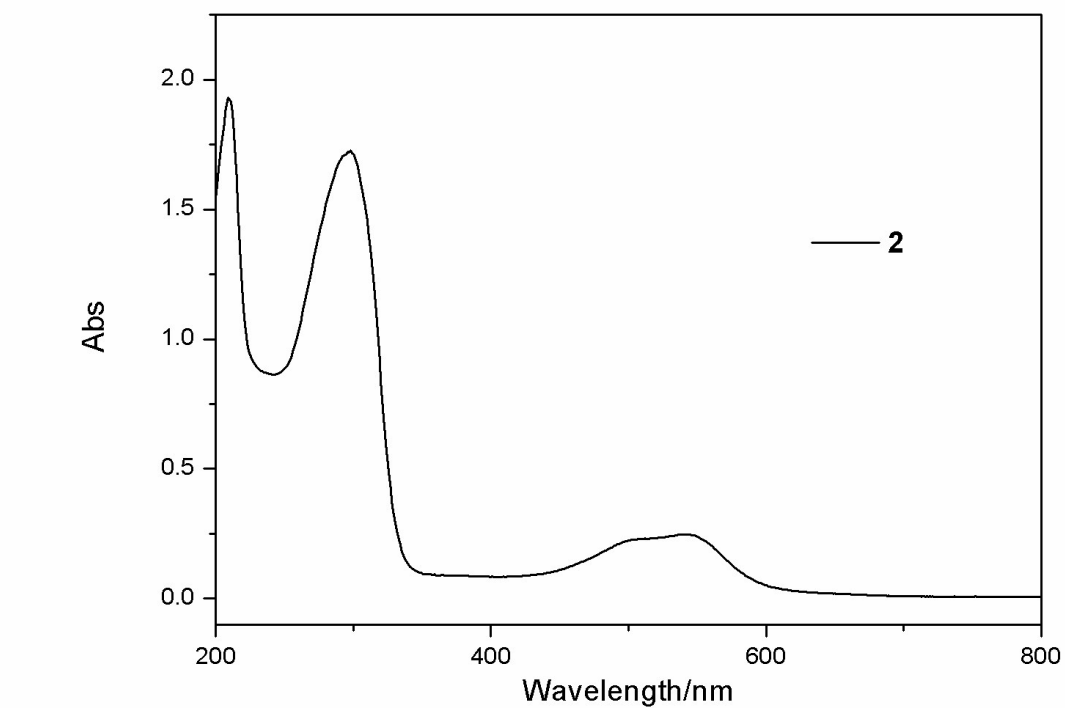

Figure S6. UV/Vis spectrum of **2** at room temperature in CH_3CN solution (10^{-5} mol·L^{-1}).

5. Thermogravimetric analyses (TGA)

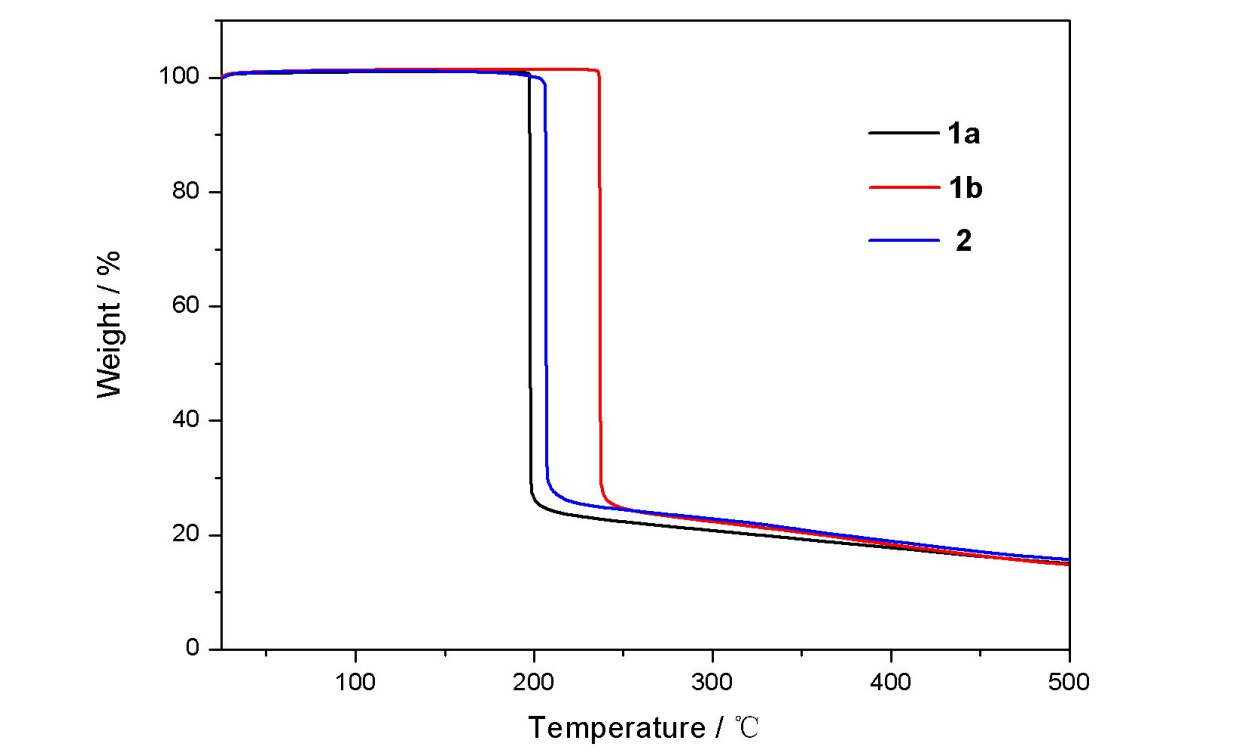

Figure S7. Thermogravimetric analyses (TGA) of **1a**, **1b** and **2**.

The weight of all three were nearly a constant following the increasing temperature until 197 °C for **1a**, 236 °C for **1b** and 206 °C for **2**, and then the complex started to decompose with abrupt losses of almost weight (76 percent for **1a**, 74 percent for **1b** and 71 percent for **2**). Further heated to 500 °C, there were approximate 14 percent of weight residual, which possibly corresponded to the iron oxides.

6. Crystal-packing diagram of complexes 1a, 1b and 2

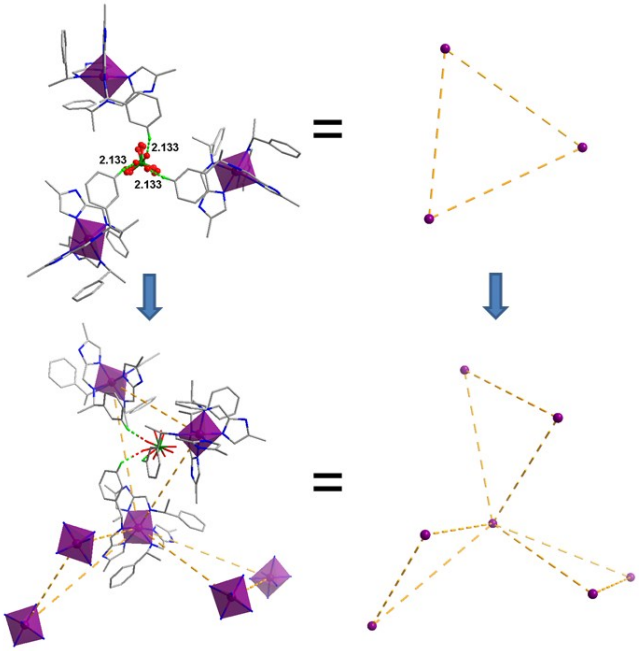

Figure S8. Representation of the crystal packing for **1a**. All H atoms and the N-alkyl chains in imidazole rings have been removed for clarity. Color code: C, gray; N, blue; Fe, violet; O, red; Cl, dark green; H-bonding interactions, green dashed lines.

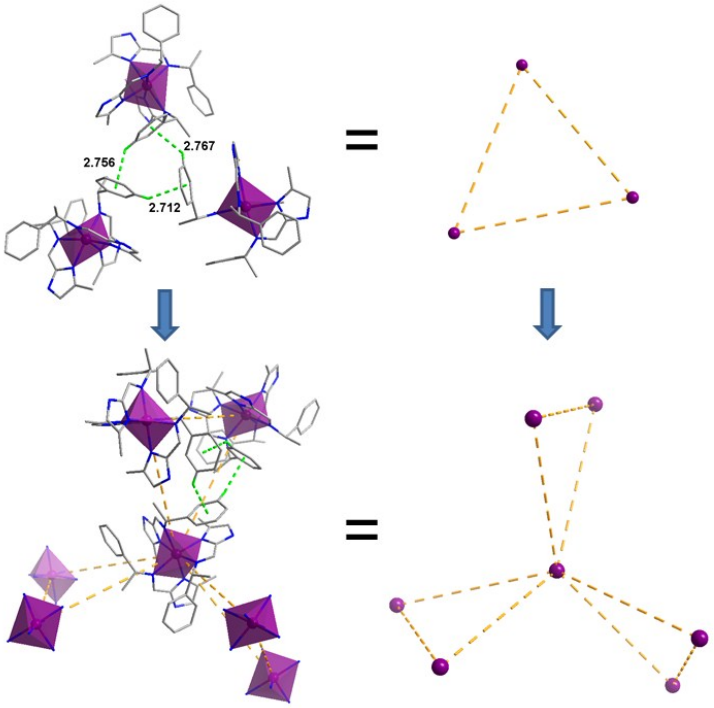

Figure S9. Representation of the crystal packing for **1b**. All H atoms, anions and the N-alkyl chains in imidazole rings have been removed for clarity. Color code: C, gray; N, blue; Fe, violet; C-H···π interactions, green dashed lines.

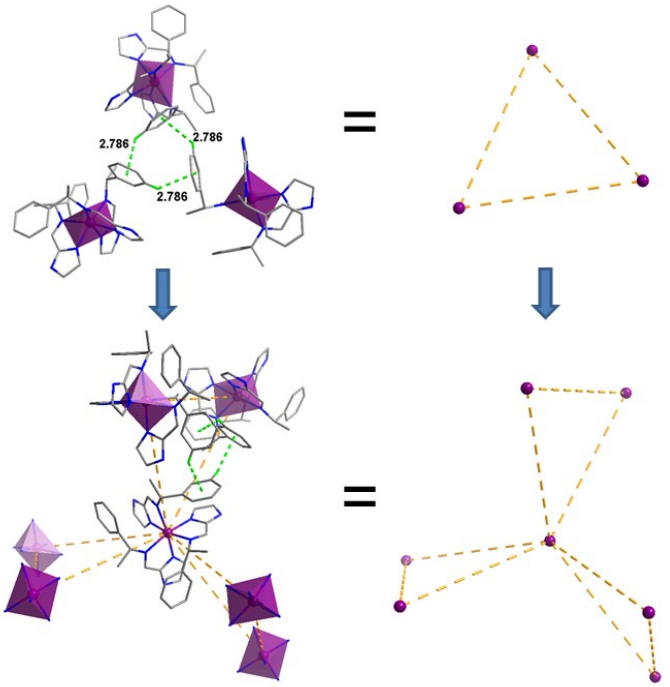

Figure S10. Representation of the crystal packing for **2**. All H atoms, anions and the N-alkyl chains in imidazole rings have been removed for clarity. Color code: C, gray; N, blue; Fe, violet; C-H···π interactions, green dashed lines.

7. Powder X-ray diffraction (PXRD) of complexes 1a, 1b and 2

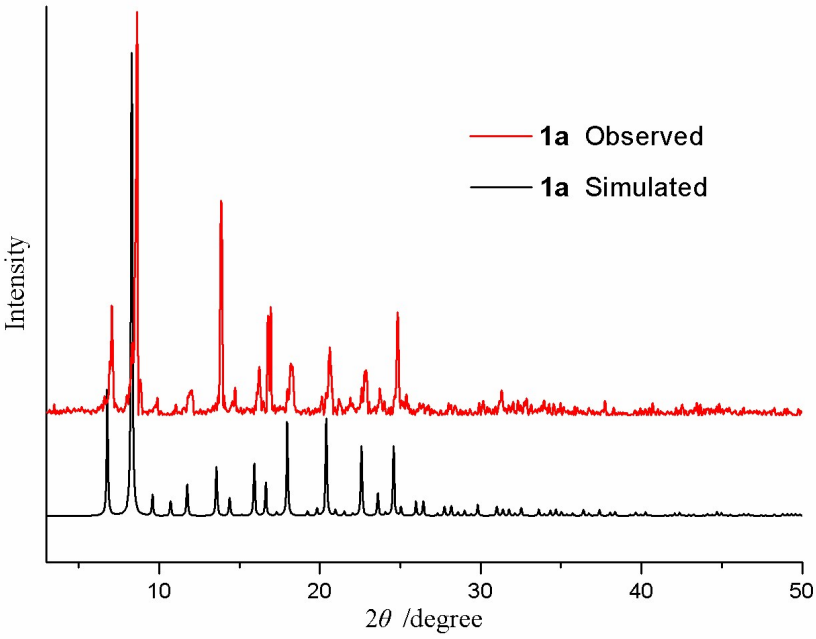

Figure S11. Observed and simulated powder X-ray diffraction (PXRD) of **1a**.

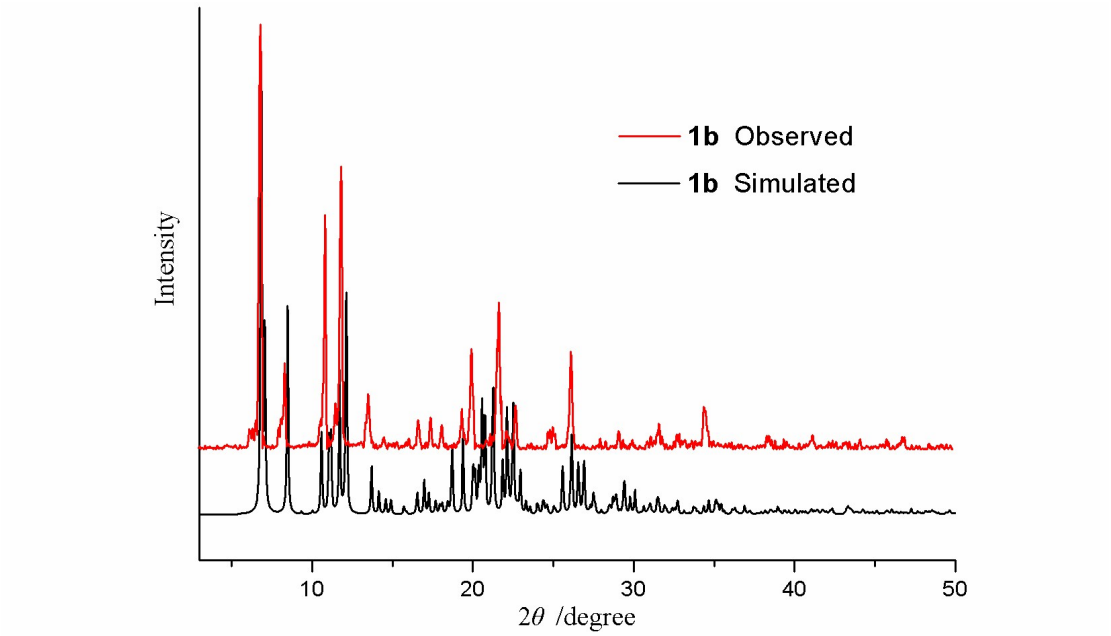

Figure S12. Observed and simulated powder X-ray diffraction (PXRD) of **1b**.

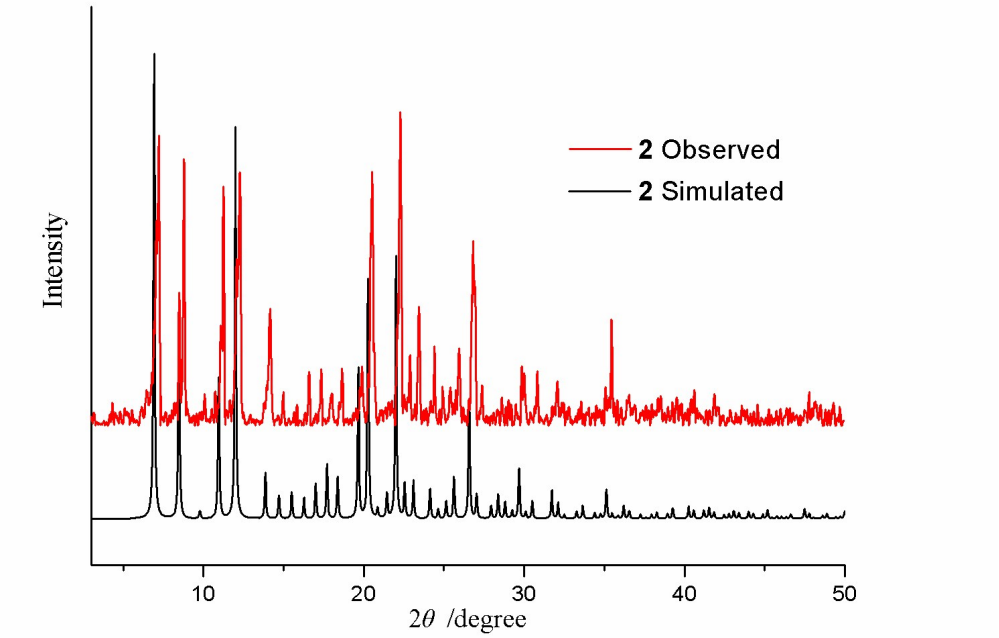

Figure S13. Observed and simulated powder X-ray diffraction (PXRD) of **2**.

8. X-ray crystallographic data

Table S1. Selected bond lengths [Å] and angles [°] for **1a**, **1b** and **2**.

1a		**1b**		**2**	
Fe(1)-N(1)	1.960(6)	Fe(1)-N(1A)	2.140(9)	Fe(1)-N(1)#5	2.096(6)
Fe(1)-N(1)#4	1.960(6)	Fe(1)-N(1B)	2.151(10)	Fe(1)-N(1)#6	2.096(6)
Fe(1)-N(1)#3	1.960(6)	Fe(1)-N(1C)	2.168(9)	Fe(1)-N(1)	2.096(6)
Fe(1)-N(3)	1.982(7)	Fe(1)-N(3B)	2.204(9)	Fe(1)-N(3)	2.196(6)
Fe(1)-N(3)#4	1.982(7)	Fe(1)-N(3C)	2.208(9)	Fe(1)-N(3)#5	2.196(6)
Fe(1)-N(3)#3	1.982(7)	Fe(1)-N(3A)	2.237(9)	Fe(1)-N(3)#6	2.196(6)
N(1)-Fe(1)-N(1)#4	91.3(2)	N(1A)-Fe(1)-N(1B)	94.2(4)	N(1)#5-Fe(1)-N(1)#6	90.5(2)
N(1)-Fe(1)-N(1)#3	91.3(2)	N(1A)-Fe(1)-N(1C)	94.5(4)	N(1)#5-Fe(1)-N(1)	90.5(2)
N(1)#4-Fe(1)-N(1)#3	91.3(2)	N(1B)-Fe(1)-N(1C)	92.5(4)	N(1)#6-Fe(1)-N(1)	90.5(2)
N(1)-Fe(1)-N(3)	81.0(3)	N(1A)-Fe(1)-N(3B)	169.6(4)	N(1)#5-Fe(1)-N(3)	167.7(2)
N(1)#4-Fe(1)-N(3)	91.8(2)	N(1B)-Fe(1)-N(3B)	76.6(4)	N(1)#6-Fe(1)-N(3)	91.4(2)
N(1)#3-Fe(1)-N(3)	171.8(3)	N(1C)-Fe(1)-N(3B)	91.0(4)	N(1)-Fe(1)-N(3)	77.3(2)
N(1)-Fe(1)-N(3)#4	171.8(3)	N(1A)-Fe(1)-N(3C)	90.0(4)	N(1)#5-Fe(1)-N(3)#5	77.3(2)
N(1)#4-Fe(1)-N(3)#4	81.0(3)	N(1B)-Fe(1)-N(3C)	168.7(4)	N(1)#6-Fe(1)-N(3)#5	167.7(2)
N(1)#3-Fe(1)-N(3)#4	91.8(2)	N(1C)-Fe(1)-N(3C)	76.6(3)	N(1)-Fe(1)-N(3)#5	91.4(2)
N(3)-Fe(1)-N(3)#4	96.3(3)	N(3B)-Fe(1)-N(3C)	99.9(4)	N(3)-Fe(1)-N(3)#5	100.89(17)
N(1)-Fe(1)-N(3)#3	91.8(2)	N(1A)-Fe(1)-N(3A)	77.0(4)	N(1)#5-Fe(1)-N(3)#6	91.4(2)
N(1)#4-Fe(1)-N(3)#3	171.8(3)	N(1B)-Fe(1)-N(3A)	91.3(4)	N(1)#6-Fe(1)-N(3)#6	77.3(2)
N(1)#3-Fe(1)-N(3)#3	81.0(3)	N(1C)-Fe(1)-N(3A)	170.9(3)	N(1)-Fe(1)-N(3)#6	167.7(2)
N(3)-Fe(1)-N(3)#3	96.3(3)	N(3B)-Fe(1)-N(3A)	97.9(3)	N(3)-Fe(1)-N(3)#6	100.89(17)
N(3)#4-Fe(1)-N(3)#3	96.3(3)	N(3C)-Fe(1)-N(3A)	99.9(3)	N(3)#5-Fe(1)-N(3)#6	100.89(17)

Symmetry transformations used to generate equivalent atoms for **1a**: #3 -z+1,x+1/2,-y+3/2; #4 y-1/2,-z+3/2,-x+1; for **2**: #5 -y+1/2,-z+1,x+1/2 #6 z-1/2,-x+1/2,-y+1

9. DFT calculations

Table S2. DFT calculated energy of different spin states for **1a**, **1b** and **2**.

	1a	**1b**	**2**
E_{HS} / a.u.	-2836.70949	-2836.74990	-2718.37369
E_{LS} / a.u.	-2836.74154	-2836.70034	-2718.36454
$\Delta E_{HS\text{-}LS}$ / kJ mol^{-1}	84.15	-130.10	-24.03

$\Delta E_{HS\text{-}LS}$ in negative value means high-spin state is more stable.